Antiviral Research 202 (2022) 105311

Contents lists available at ScienceDirect

Antiviral Research

journal homepage: www.elsevier.com/locate/antiviral

HIV protease inhibitors Nelfinavir and Lopinavir/Ritonavir markedly improve lung pathology in SARS-CoV-2-infected Syrian hamsters despite lack of an antiviral effect

Caroline S. Foo [a,1], Rana Abdelnabi [a,1], Suzanne J.F. Kaptein [a], Xin Zhang [a], Sebastiaan ter Horst [a], Raf Mols [b], Leen Delang [a], Joana Rocha-Pereira [a], Lotte Coelmont [a], Pieter Leyssen [a], Kai Dallmeier [a], Valentijn Vergote [a], Elisabeth Heylen [a], Laura Vangeel [a], Arnab K. Chatterjee [c], Pieter P. Annaert [b], Patrick F. Augustijns [b], Steven De Jonghe [a], Dirk Jochmans [a], Mieke Gouwy [d], Seppe Cambier [d], Jennifer Vandooren [e], Paul Proost [d], Christine van Laer [f,g], Birgit Weynand [h], Johan Neyts [a,i,*]

[a] KU Leuven Department of Microbiology, Immunology and Transplantation, Rega Institute for Medical Research, Laboratory of Virology and Chemotherapy, B-3000, Leuven, Belgium
[b] KU Leuven, Department of Pharmaceutical and Pharmacological Sciences, Drug Delivery & Disposition, Box 921, 3000, Leuven, Belgium
[c] Calibr at Scripps Research, La Jolla, CA, USA
[d] KU Leuven Department of Microbiology, Immunology and Transplantation, Rega Institute for Medical Research, Laboratory of Molecular Immunology, B-3000, Leuven, Belgium
[e] KU Leuven Department of Microbiology, Immunology and Transplantation, Rega Institute for Medical Research, Laboratory of Immunobiology, B-3000, Leuven, Belgium
[f] Clinical Department of Laboratory Medicine, University Hospital Leuven, Leuven, Belgium
[g] Department of Cardiovascular Sciences, Centre for Molecular and Vascular Biology, KU Leuven, Leuven, Belgium
[h] KU Leuven Department of Imaging and Pathology, Division of Translational Cell and Tissue Research, B-3000, Leuven, Belgium
[i] GVN, Global Virus Network, Baltimore, MD, USA

A B S T R A C T

Nelfinavir is an HIV protease inhibitor that has been widely prescribed as a component of highly active antiretroviral therapy, and has been reported to exert *in vitro* antiviral activity against SARS-CoV-2. We here assessed the effect of Nelfinavir in a SARS-CoV-2 infection model in hamsters. Despite the fact that Nelfinavir, [50 mg/kg twice daily (BID) for four consecutive days], did not reduce viral RNA load and infectious virus titres in the lung of infected animals, treatment resulted in a substantial improvement of SARS-CoV-2-induced lung pathology. This was accompanied by a dense infiltration of neutrophils in the lung interstitium which was similarly observed in non-infected hamsters. Nelfinavir resulted also in a marked increase in activated neutrophils in the blood, as observed in non-infected animals. Although Nelfinavir treatment did not alter the expression of chemoattractant receptors or adhesion molecules on human neutrophils, *in vitro* migration of human neutrophils to the major human neutrophil attractant CXCL8 was augmented by this protease inhibitor. Nelfinavir appears to induce an immunomodulatory effect associated with increasing neutrophil number and functionality, which may be linked to the marked improvement in SARS-CoV-2 lung pathology independent of its lack of antiviral activity. Since Nelfinavir is no longer used for the treatment of HIV, we studied the effect of two other HIV protease inhibitors, namely the combination Lopinavir/Ritonavir (Kaletra™) in this model. This combination resulted in a similar protective effect as Nelfinavir against SARS-CoV2 induced lung pathology in hamsters.

1. Introduction

Severe acute respiratory syndrome coronavirus 2 (SARS-CoV-2) caused more than 6 million deaths within the time-span of 23 months after its discovery (WHO Coronavirus Disease (COVID-19) Dashboard, 2022). SARS-CoV-2-induced COVID-19 is mainly an inflammatory

* Corresponding author. KU Leuven Department of Microbiology, Immunology and Transplantation, Rega Institute for Medical Research, Laboratory of Virology and Chemotherapy, B-3000, Leuven, Belgium.
E-mail address: johan.neyts@kuleuven.be (J. Neyts).
[1] these authors contributed equally.

https://doi.org/10.1016/j.antiviral.2022.105311
Received 10 February 2022; Received in revised form 24 March 2022; Accepted 26 March 2022
Available online 4 April 2022

disease that displays a variety of symptoms including fever, dry cough, muscle weakness, loss of sense of taste and smell, and diarrhoea (Tay et al., 2020). In some patients, the disease is accompanied with a massive cytokine storm and exaggerated immune response, resulting in severe complications such as acute respiratory distress syndrome (ARDS), respiratory failure, septic shock and multi-organ failure (Tay et al., 2020).

Nelfinavir mesylate (Viracept) is an FDA-approved HIV-protease inhibitor (PI) (Kaldor et al., 1997). By inhibiting the HIV-1 protease, it prevents the cleavage of viral Gag and Gag-Pol polyproteins, resulting in immature and non-infectious virus particles (Kaplan et al., 1993; Peng et al., 1989). Nelfinavir has been reported to result in some *in vitro* inhibitory activity against SARS-CoV-2 (Ianevski et al., 2020; Yamamoto et al., 2020). Additionally, inhibition of SARS-CoV-2 Spike glycoprotein mediated cell-fusion has been reported (Musarrat et al., 2020) and *in silico* docking studies predict binding of Nelfinavir for the catalytic site of the SARS-CoV-2 main protease, M^{pro} (Bolcato et al., 2020; Xu et al., 2020; Huynh et al., 2020). We here wanted to assess whether Nelfinavir results in an antiviral effect against SARS-CoV-2 in Syrian hamsters. High viral titres are reached in the lung upon infection and the animals develop a COVID-like lung pathology (Boudewijns et al., 2020; Kaptein et al., 2020). The model is well-suited to assess the impact of antiviral drugs as we and others have demonstrated. Notably, we have demonstrated that Favipiravir and Molnupiravir (EIDD-2801) markedly reduce SARS-CoV-2 replication in hamsters, including against variants of concern (Abdelnabi et al., 2021; Kaptein et al., 2020). We here report that although Nelfinavir does not result in an antiviral effect in the hamster model, it has a protective effect against virus-induced pathology. Since Nelfinavir is no longer in clinical use in the EU, we next explored whether the fixed dose HIV protease combination Lopinavir and ritonavir (Kaletra™) results in a similar effect. Lopinavir/Ritonavir (Kaletra™) is an antiretroviral therapy approved for the treatment of HIV, in which Ritonavir increases the bioavailability of Lopinavir by preventing its metabolization by host cytochrome P450 3A4 (Kempf et al., 1997; Sham et al., 1998). Lopinavir has demonstrated antiviral activity *in vitro* against coronaviruses SARS-CoV and MERS-CoV (Chu et al., 2004; de Wilde et al., 2014), and more recently, SARS-CoV-2 (Choy et al., 2020). We report that similar to Nelfinavir, Lopinavir/Ritonavir results in a protective effect against virus-induced pathology in the hamster model despite the lack of an antiviral activity.

2. Materials and methods

2.1. SARS-CoV-2 strain

The SARS-CoV-2 strain used in this study, BetaCov/Belgium/GHB-03021/2020 (EPI ISL 109 407976|2020-02-03), was recovered from a nasopharyngeal swab taken from an RT-qPCR confirmed asymptomatic patient who returned from Wuhan, China in the beginning of February 2020. A close relation with the prototypic Wuhan-Hu-1 2019-nCoV (GenBank accession 112 number MN908947.3) strain was confirmed by phylogenetic analysis. Infectious virus was isolated by serial passaging on HuH7 and Vero E6 cells (Kaptein et al., 2020); passage 6 virus was used for the study described here. The titre of the virus stock was determined by end-point dilution on Vero E6 cells by the Reed and Muench method (Reed and Muench, 1938). Live virus-related work was conducted in the high-containment A3 and BSL3+ facilities of the KU Leuven Rega Institute (3CAPS) under licenses AMV 30112018 SBB 219 2018 0892 and AMV 23102017 SBB 219 20170589 according to institutional guidelines.

2.2. Cells

Vero E6 cells (African green monkey kidney, ATCC CRL-1586) were cultured in minimal essential medium (Gibco) supplemented with 10% fetal bovine serum (FCS; Integro), 1% L-glutamine (Gibco) and 1% bicarbonate (Gibco). End-point titrations were performed with medium containing 2% FCS instead of 10%.

2.3. SARS-CoV-2 infection model in hamsters

The hamster infection model of SARS-CoV-2 has been described before (Kaptein et al., 2020). In brief, wild-type, female Syrian Golden hamsters (*Mesocricetus auratus*) of 6–8 weeks old weighing 90–120 g were purchased from Janvier Laboratories and were housed per two in ventilated isolator cages (IsoCage N Biocontainment System, Tecniplast) with ad libitum access to food and water and cage enrichment (wood block). The animals were acclimated for 4 days prior to study start. Housing conditions and experimental procedures were approved by the ethics committee of animal experimentation of KU Leuven (license P065-2020). Female hamsters of 6–8 weeks old were anesthetized with ketamine/xylazine/atropine and inoculated intranasally with 50 μL containing 2×10^6 TCID50 SARS-CoV-2 (day 0).

2.4. Study design

At day 0, animals were treated twice daily with an intraperitoneal injection (i.p.) of 15 mg/kg or 50 mg/kg of Nelfinavir (purchased from MedChem Express, formulated in 5% DMSO-5% PEG-400 and 5% Tween-80 in PBS to a stock of 5 mg/ml and 10 mg/ml, respectively) or vehicle control (5% DMSO-5% PEG-400 and 5% Tween-80 in PBS) just before infection with SARS-CoV-2. For the Lopinavir/Ritonavir study, animals were treated once daily with Lopinavir by i.p. injection and Ritonavir by oral gavage. Both Lopinavir and Ritonavir were formulated in 43% ethanol, 27% propylene glycol in water to a stock of 30 mg/ml and 20 mg/ml, respectively. Treatments continued until day 3 pi. During this time, hamsters were monitored for appearance, behavior, and weight. At day 4 pi, hamsters were euthanized by i.p. injection of 500 μL Dolethal (200 mg/ml sodium pentobarbital, Vétoquinol SA) at about 16 h after the last dose. Lungs were collected and viral RNA for N-protein and infectious virus were quantified by RT-qPCR and end-point virus titration, respectively. For the therapeutic setting, animals were treated twice daily with i.p. administration of 50 mg/kg of Nelfinavir or vehicle control 1 day after infection with SARS-CoV-2. Treatments continued until day 4 pi, and hamsters were euthanized at day 5 pi. Non-infected hamsters were treated twice daily with i.p. administration of 50 mg/kg of Nelfinavir or vehicle control from day 0 to day 3 (for 4 days) before euthanasia on day 4. Whole blood was collected in EDTA-coated collection tubes for automated hematological analysis.

For quantification of Nelfinavir plasma levels, blood was collected by cardiac puncture in EDTA-blood tubes and plasma was collected after centrifugation at 10 000 g for 10 min.

2.5. SARS-CoV-2 RT-qPCR

Hamster lung tissues were collected after sacrifice and were homogenized using bead disruption (Precellys) in 350 μL RLT buffer (RNeasy Mini kit, Qiagen) and centrifuged (10.000 rpm for 5 min) to pellet the cell debris. RNA was extracted according to the manufacturer's instructions. Of 50 μL eluate, 4 μL was used as a template in RT-qPCR reactions. RT-qPCR was performed on a LightCycler96 platform (Roche) using the iTaq Universal Probes One-Step RT-qPCR kit (BioRad) with N2 primers and probes targeting the nucleocapsid (Primer 1: 5′-TTA CAA ACA TTG GCC GCA AA-3′, Primer 2: 5′-GCG CGA CAT TCC GAA GAA-3′, Probe: 5′-FAM-ACA ATT TGC CCC CAG CGC TTC AG-BHQ1-3′) (Kaptein et al., 2020). Standards of SARS-CoV-2 cDNA (IDT) were used to express viral genome copies per mg tissue or per mL serum.

2.6. End-point virus titrations

Lung tissues were homogenized using bead disruption (Precellys) in 350 μL minimal essential medium and centrifuged (10000 rpm for 5min

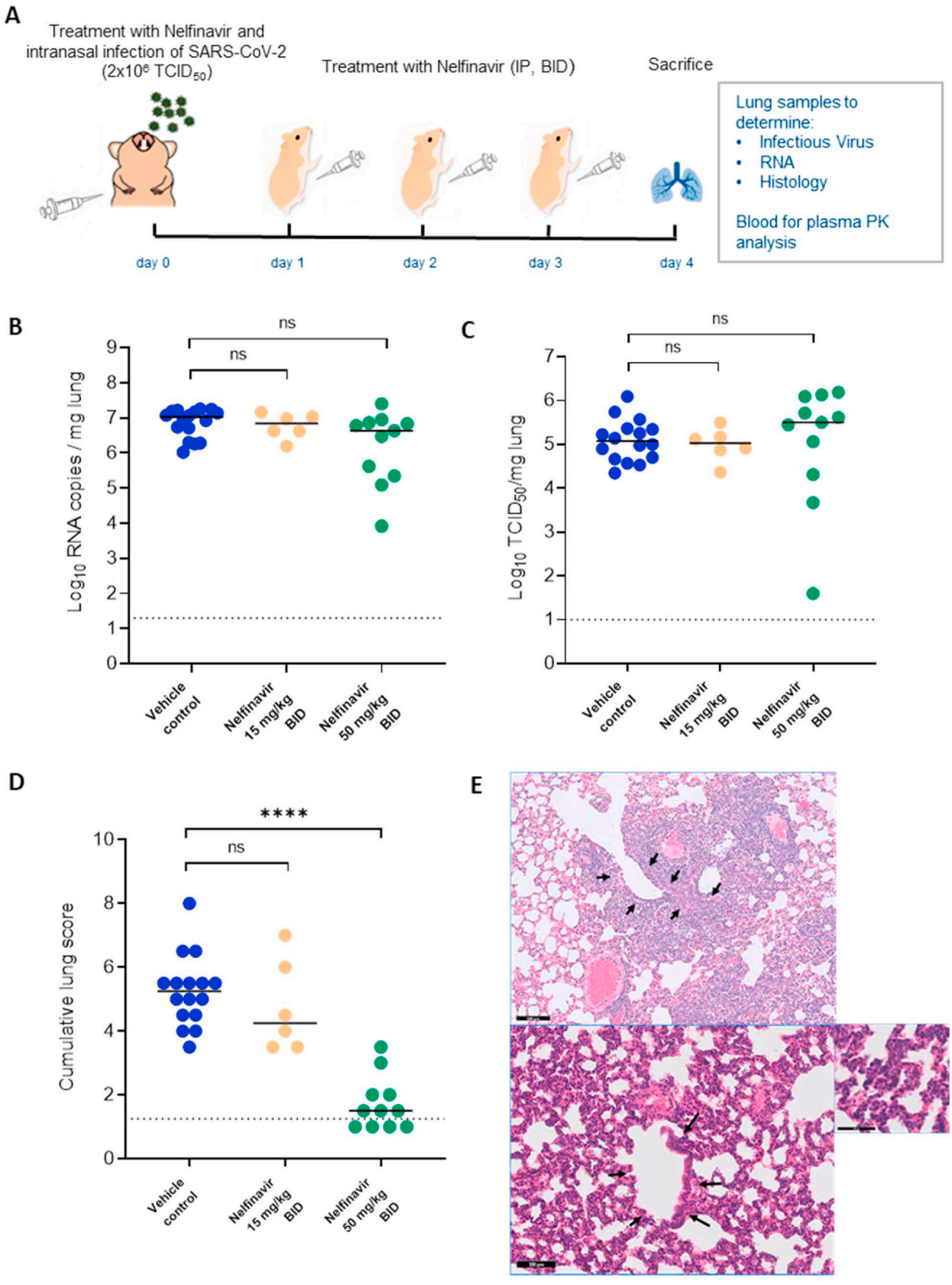

(caption on next page)

Fig. 1. Nelfinavir markedly improves lung pathology of SARS-CoV-2-infected Syrian hamsters despite lack of antiviral efficacy when administered at the time of infection. (A) Set-up of the study. **(B)** Viral RNA levels in the lungs of hamsters treated with vehicle (control), 15 mg/kg Nelfinavir BID, or 50 mg/kg Nelfinavir BID at 4 dpi expressed as $\log_{10}$ SARS-CoV-2 RNA copies per mg lung tissue. Individual data and median values are presented. **(C)** Infectious virus titres in the lungs of hamsters treated with vehicle (control), 15 mg/kg Nelfinavir BID, or 50 mg/kg Nelfinavir BID at 4 dpi expressed as $\log_{10}$ $TCID_{50}$ per mg lung tissue. Individual data and median values are presented. **(D)** Cumulative severity score from H&E-stained slides of lungs from SARS-CoV-2-infected hamsters at 4 dpi treated with vehicle, 15 mg/kg Nelfinavir BID, or 50 mg/kg Nelfinavir BID. Individual datapoints and lines indicating median values are presented. The dotted line represents the median lung score in healthy, untreated, non-infected animals. (E) Representative H&E-stained slides of lungs from vehicle control (top panel) and 50 mg/kg BID Nelfinavir-treated (bottom panel) SARS-CoV-2-infected hamsters at 4 dpi. Top panel: bronchopneumonia centred on a bronchiol (black arrows) in a vehicle-treated hamster (scale bar at 100 μm). Bottom panel: severe interstitial inflammation with mostly PMN and congestion in a Nelfinavir-treated hamster (scale bar at 100 μm). Black arrows indicate bronchiol (insert at higher magnification, scale bar at 50 μm). Data for 15 mg/kg Nelfinavir are from one study (n = 6), and data for 50 mg/kg Nelfinavir are from two independent experiments (n = 11). Data were analyzed using the Mann-Whitney *U* test. ns indicates non-significant; ****P < 0.0001.

at 4 °C) to pellet the cell debris. To quantify infectious SARS-CoV-2 particles, endpoint titrations were performed on confluent Vero E6 cells in 96- well plates. Viral titres were calculated by the Reed and Muench method (Reed and Muench, 1938) using the Lindenbach calculator and were expressed as 50% tissue culture infectious dose ($TCID_{50}$) per mg tissue.

2.7. Histology

For histological examination, the lungs were fixed overnight in 4% formaldehyde and embedded in paraffin. Tissue sections (5 μm) were analyzed after staining with hematoxylin and eosin and scored blindly for lung damage by an expert pathologist. The scored parameters, to which a cumulative score of 1–9 was attributed, were the following: congestion, intra-alveolar hemorrhagic, apoptotic bodies in bronchus wall, necrotizing bronchiolitis, perivascular edema, bronchopneumonia, perivascular inflammation, peribronchial inflammation and vasculitis.

2.8. Blood cell count analysis

Whole blood EDTA samples were analyzed on Sysmex XN-9100™ analyzer (Sysmex, Kobe, Japan) with the prediluted mode within a few hours after blood collection. This prediluted procedure requires a manual predilution of the whole blood samples, namely 50 μL whole blood and 300 μL Cellpack DCL. Samples were checked for *in vitro* clot formation, if a clot was present the results for leukocytes, erythrocytes and platelets were excluded for further analysis. Both results of conventional and research hematological parameters were interpreted. For every sample, a blood smear was manually made and stained with automated slide stainer SP-50 (Sysmex, Kobe, Japan) with the May Grünwald – Giemsa staining. All samples were microscopically evaluated with a DI-60 digital cell imaging analyzer for leukocytes differentiation.

2.9. Isolation of peripheral blood human neutrophils and flow cytometry

Neutrophils were isolated from fresh blood of healthy donors by immuno-magnetic negative selection (EasySep™ Direct Human Neutrophil Isolation Kit; Stemcell Technologies, Vancouver, Canada). Purified human neutrophils were treated with Nelfinavir (50 μg/ml) or vehicle control for 1 h at 37 °C and were then subjected to flow cytometry analysis for evaluation of expression of adhesion molecules and chemoattractant receptors. Neutrophils were treated with FcR block (Miltenyi Biotec, Bergisch Gladbach, Germany) and Fixable Viability Stain 620 (BD Biosciences) or Zombie Aqua 516 (Biolegend, San Diego, CA) during 15 min at room temperature. Subsequently, cells were washed with flow cytometry buffer [PBS + 2% (v/v) FCS + 2 mM EDTA] and stained with fluorescently labeled antibodies. Following incubation for 25 min (on ice), cells were washed with flow cytometry buffer and fixed with BD Cytofix (BD Biosciences). Results were analyzed using a BD LSRFortessa™ X-20 (BD Biosciences) equipped with DIVA software (BD Biosciences). FlowJo software (BD Biosciences) was used for downstream analysis. Neutrophils were gated as $CD16^+CD66b^+$ cells within the population of living single cells.

2.10. Evaluation of proteolytic activity

Neutrophils were isolated from fresh blood of healthy donors via density gradient centrifugation and were suspended in degranulation buffer (120 mM NaCl, 15 mM $CaCl_2$, 20 mM Tris/HCl pH 7.5) at a concentration of 10^7 cells/ml. neutrophil degranulation was induced by adding N-formyl-methionyl-leucyl-phenylalanine (fMLF) (0.5 μM) for 20 min at 37 °C. The supernatant containing human neutrophil proteases was collected by centrifugation. Neutrophil degranulates were incubated with indicated concentrations of Nelfinavir or a control condition containing the equivalent concentration of DMSO (Nelfinavir solvent) for 10 min at 37 °C. Next, the remaining protease activity was determined using the following fluorogenic protease substrates: Mca-PLGL-Dpa-AR-NH_2 [OmniMMP, substrate for matrix metalloproteinases (MMPs), ADAM17/TACE, Cathepsin D (aspartic protease) and Cathepsin E (aspartic protease)], dye quenched-gelatin (cleaved by gelatinases such as neutrophil elastase, MMP-2, MMP-9).

2.11. In vitro Boyden microchamber assay

Briefly, neutrophils were purified by density gradient centrifugation and erythrocytes removed by hypotonic shock (Metzemaekers et al., 2021). Purified neutrophils were pre-stimulated (1 h at 37 °C) with vehicle control or Nelfinavir (20 or 50 μg/ml) and subsequently added to the upper compartment of the Boyden microchamber. In the lower compartment the human CXC chemokine CXCL8 (Peprotech, Rocky Hill, CT) was added, at dilutions of 5 or 15 ng/ml in Boyden chamber buffer (1xHBSS + 0.5% human serum albumin). The Boyden chamber was incubated at 37 °C for 45 min. Cells were fixed on the membrane and migrated cells were counted by light microscopy (500x). The chemotactic index was calculated by dividing the number of migrated cells to CXCL8 to the number of migrated cells towards the corresponding buffer.

2.12. Statistics

GraphPad Prism (GraphPad Software, Inc.) was used to perform statistical analysis. Statistical significance was determined using the non-parametric Mann Whitney *U* test. P-values of <0.05 were considered significant.

3. Results

3.1. Nelfinavir improves lung pathology of SARS-CoV-2-infected hamsters when administered at the time of infection without an effect on viral load in the lungs

To evaluate the antiviral efficacy of Nelfinavir against SARS-CoV-2 in hamsters, six to eight weeks old female Syrian Golden hamsters were treated with Nelfinavir (15 mg/kg/dose or 50 mg/kg/dose) or the vehicle control, by intraperitoneal injection (IP) within 1 h before

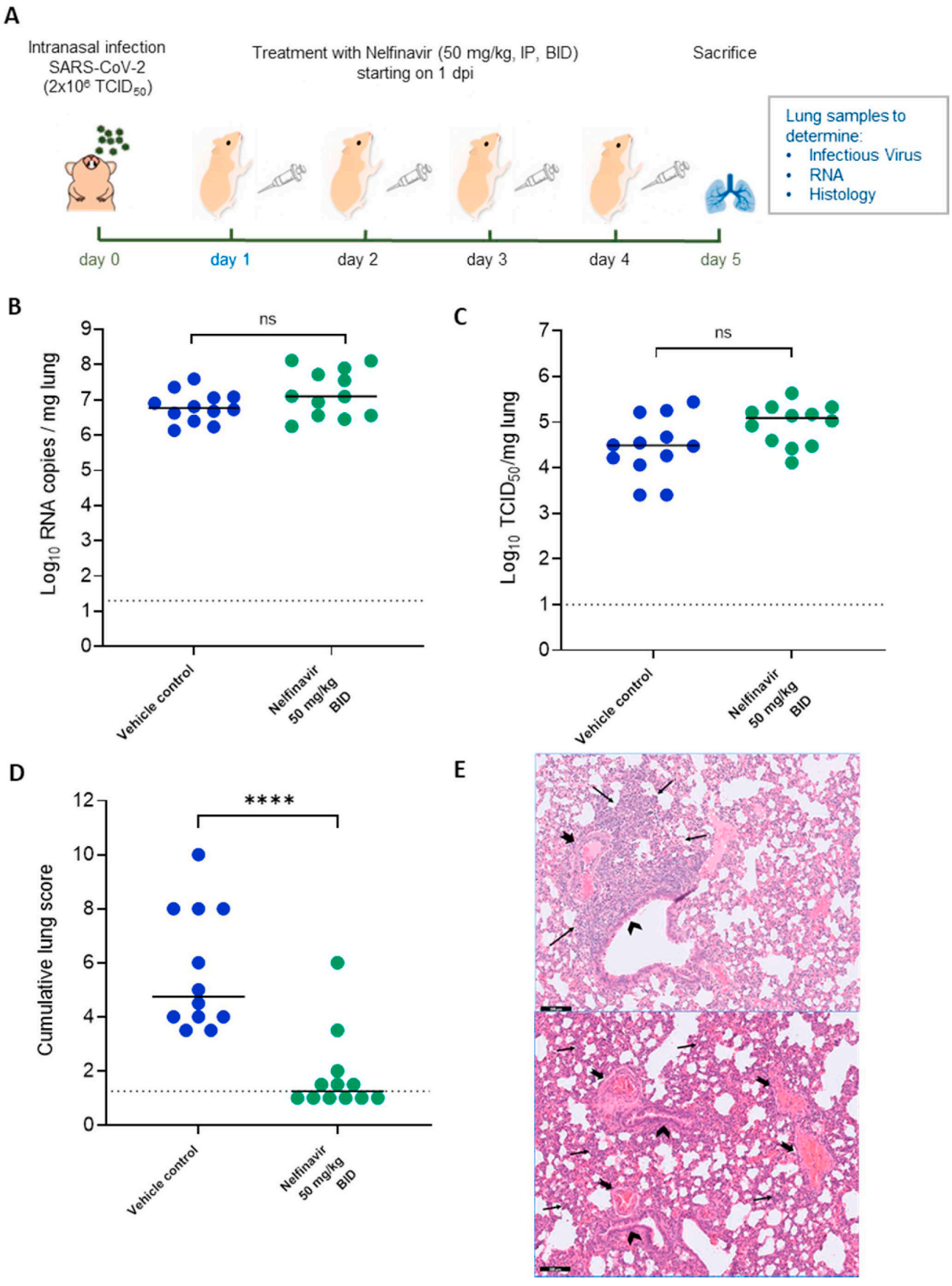

(caption on next page)

Fig. 2. Delayed administration of Nelfinavir markedly improves lung pathology of SARS-CoV-2-infected Syrian hamsters despite lack of antiviral efficacy in this therapeutic setting. (A) Set-up of the study. **(B)** Viral RNA levels in the lungs of hamsters treated with vehicle (control) or 50 mg/kg Nelfinavir BID at 5 dpi expressed as $\log_{10}$ SARS-CoV-2 RNA copies per mg lung tissue. Individual data and median values are presented. **(C)** Infectious virus titres in the lungs of hamsters treated with vehicle (control) or 50 mg/kg Nelfinavir BID at 5 dpi expressed as $\log_{10}$ $TCID_{50}$ per mg lung tissue. Individual data and median values are presented. **(D)** Cumulative severity score from H&E-stained slides of lungs from SARS-CoV-2-infected hamsters at 5 dpi treated with vehicle or 50 mg/kg Nelfinavir BID. Individual datapoints and lines indicating median values are presented. The dotted line represents the median lung score in healthy, untreated, non-infected animals. (E) Representative H&E-stained slides of lungs from vehicle control (top panel) and 50 mg/kg BID Nelfinavir-treated (bottom panel) SARS-CoV-2-infected hamsters at 5 dpi. Top panel: area of bronchopneumonia (small arrows); peri-bronchial (arrowhead) and perivascular (arrows) inflammation with endothelialitis in a vehicle-treated hamster (scale bar at 100 μm). Bottom panel: interstitium filled with neutrophils (small arrows), no alveolar, bronchial (arrowhead) or vascular (arrows) inflammation in a Nelfinavir-treated hamster (scale bar at 100 μm). Data are from two independent experiments (n = 12). Data were analyzed using the Mann-Whitney *U* test. ns indicates non-significant; ****P < 0.0001.

intranasal infection with 50 μL SARS-CoV-2 [2×10^6 $TCID_{50}$ BetaCov/Belgium/GHB-03021/2020] (Fig. 1A). The drug, as well as the vehicle control, were administered twice daily for four consecutive days. At day four post-infection, lungs were collected at end-point sacrifice (day 4 p.i) for viral RNA load and infectious virus titres quantification as well as lung histopathology as previously described (Kaptein et al., 2020). Groups treated with either 15 mg/kg BID or 50 mg/kg BID Nelfinavir had comparable levels of lung viral RNA load and infectious virus titres as the vehicle control group (data from two independent studies) (Fig. 1B and C), indicating a lack of *in vivo* antiviral efficacy of Nelfinavir in this model. Intriguingly, the overall histological scoring for 50 mg/kg Nelfinavir-treated hamsters was nearly comparable to baseline scores from those of non-infected, non-treated hamsters (median score of 1.25 as indicated on Fig. 1D); thus, Nelfinavir treatment significantly improved lung pathology as compared to vehicle treatment. This remarkable protective effect of Nelfinavir treatment was accompanied by an unusual, highly dense infiltration of neutrophils in the interstitium. This was not observed in vehicle-treated hamsters (Fig. 1E). The weight change recorded at 4 dpi as compared to 0 dpi was around 0% for the 15 mg/kg BID Nelfinavir-treated group and an average weight loss of around 8% was observed in the 50 mg/kg BID Nelfinavir-treated group, which was significantly different from the average weight gain of about 2.5% in the vehicle control group (Supp Fig. 1B). This weight loss may be attributed to the gastrointestinal intolerances from signs of diarrhoea observed in the animals. It is more pronounced in the context of SARS-CoV-2 infection, with non-infected hamsters treated with Nelfinavir at 50 mg/kg BID for four days having an average weight loss of about 0.6% at day 4 compared to day 0 (Supp Fig. 1A).

3.2. Nelfinavir improves lung pathology of SARS-CoV-2-infected hamsters in a therapeutic setting without reducing viral load

To evaluate the effects of Nelfinavir in a therapeutic setting, SARS-CoV-2-infected hamsters were treated with Nelfinavir 50 mg/kg BID starting one day after infection for four days (Fig. 2A). Nelfinavir-treated animals had comparable levels of lung viral RNA load and infectious virus titres as the vehicle control group (Fig. 2B and C), confirming the lack of antiviral efficacy of Nelfinavir in this model. With delayed Nelfinavir treatment, a significant improvement in lung histopathological scoring and the unusual, highly dense infiltration of neutrophils in the interstitium was similarly observed (Fig. 2D and E). An average weight loss of around 10% was observed in the Nelfinavir-treated group at 5 dpi compared to at 0 dpi, which was significantly different compared to the vehicle control group (Supp Fig. 1C).

3.3. Nelfinavir results in an increased number of activated neutrophils in the blood and enhanced in vitro neutrophil migration

To further explore the neutrophil infiltration observed with Nelfinavir treatment, non-infected hamsters were treated with Nelfinavir 50 mg/kg BID for four days (Fig. 3A). Lung histopathological scorings of non-infected, Nelfinavir-treated animals were similar to non-infected, vehicle-treated animals (Supp Fig. 2A) at baseline scores of 1. Interstitial neutrophils were absent in the lungs of vehicle-treated animals, and present in Nelfinavir-treated animals (Supp Fig. 2A and 2B). These results indicate that Nelfinavir alone does not induce lung pathology, but rather induces the unusual infiltration of neutrophils in the lung interstitium. The impact of Nelfinavir on neutrophil levels in the blood was also examined. An average of ~170 nM Nelfinavir was measured in the plasma of 13 animals across the studies, 16 h after the last treatment at the point of sacrifice, confirming the exposure of Nelfinavir in the blood. Haematological analysis revealed increases in white blood cell, platelet, and neutrophil counts in Nelfinavir-treated, uninfected animals as compared to the vehicle control (Fig. 3B, C, D). The neutrophils of Nelfinavir-treated animals had a higher granularity intensity (Neut-GI) (Fig. 3E) and a higher reactivity intensity (Neut-RI) (Fig. 3F) compared to those of the vehicle-treated animals, whereas no differences were observed in overall neutrophil volume (Fig. 3G). These results indicate that Nelfinavir treatment induces an immunomodulatory effect involving an increase in numbers of activated neutrophils.

To further elucidate the mechanism behind this observation, we examined the effect of Nelfinavir on the expression of adhesion molecules and chemoattractant receptors on the membrane of peripheral blood human neutrophils by flow cytometry (Supp Fig. 3). Stimulation of neutrophils for 1 h with Nelfinavir had no significant effect on the surface expression of the adhesion molecules CD62L (L-selectin) and integrin CD11b compared to baseline (Supp Fig. 3A). Moreover, Nelfinavir did not significantly alter the expression of the major neutrophil chemoattractant receptors on human neutrophils, including the chemokine receptors CXCR1 and CXCR2, complement receptor C5aR and the formyl peptide receptor FPR1 over time (Supp Fig. 3B). In addition, Nelfinavir was unable to directly inhibit the proteolytic activity of the most abundant proteases secreted by stimulated human neutrophils (Supp Fig. 4). Nevertheless, Nelfinavir significantly enhanced the migration of human neutrophils towards the CXCR1 and CXCR2 agonist CXCL8 (5 and 25 ng/ml) in the Boyden microchamber assay *in vitro* (Fig. 4).

3.4. The fixed dose HIV protease inhibitor combination, Lopinavir/Ritonavir, improves lung pathology of SARS-CoV-2-infected hamsters without an effect on viral load in the lungs

To explore whether the effects observed with Nelfinavir treatment are specific to the drug, we tested another HIV protease inhibitor, Lopinavir boosted with Ritonavir, against SARS-CoV-2 in our model. SARS-CoV-2-infected hamsters were treated with Lopinavir/Ritonavir (either 40/10 mg/kg/dose or 80/20 mg/kg/dose, IP/oral) once daily within 1 h before intranasal infection with SARS-CoV-2 (Fig. 5A). As with Nelfinavir, Lopinavir/Ritonavir-treated animals did not present with a significant decrease in lung viral load compared to the control group (vehicle/Ritonavir) (Fig. 5B and C). Animals treated with 80/20 mg/kg/dose had significantly reduced lung histopathological scoring compared to the control group, to a similar level as Nelfinavir (Fig. 5D). The unusual, highly dense infiltration of neutrophils in the interstitium was observed in 8 out of 12 animals (Fig. 5E). An average weight loss of about 10% was observed in animals of the Lopinavir/Ritonavir (80/20 mg/kg/dose) group at the end of the study when compared to day 0, which was significantly different from the vehicle control group (Supp.

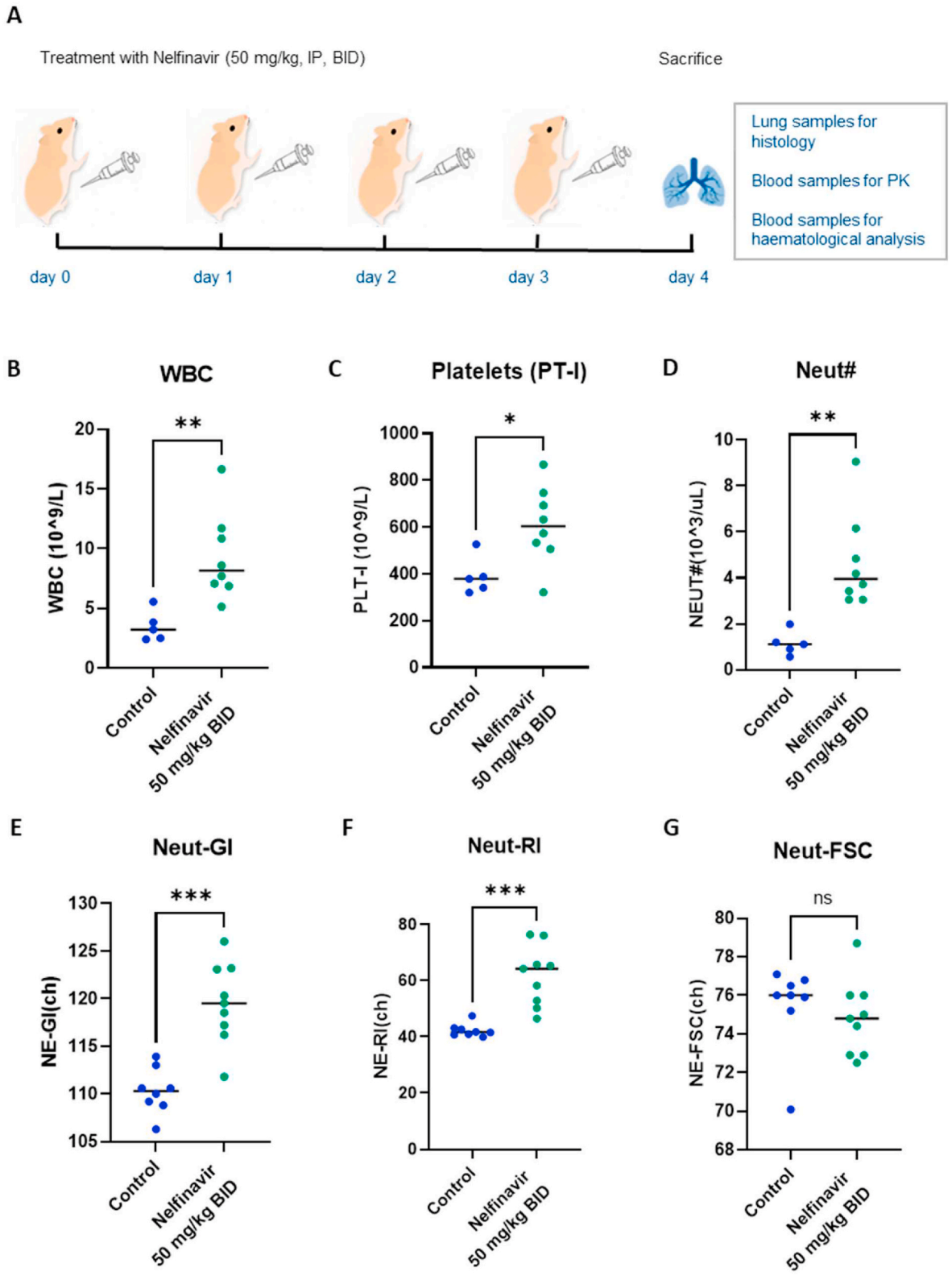

Fig. 3. Nelfinavir results in an increased number of activated neutrophils in the blood in non-infected hamsters.

Fig. 5). Gastrointestinal intolerances from signs of diarrhoea was also observed in the animals. An average of ~275 nM Lopinavir was measured in the plasma of 6 animals, 24 h–26 h after the last treatment at the point of sacrifice, confirming the exposure of Lopinavir in the blood.

4. Discussion

The initial aim of this study was to explore whether the *in vitro* antiviral activity of Nelfinavir against SARS-CoV-2 translates also in an antiviral effect in a Syrian hamster infection model. We demonstrate that Nelfinavir does not reduce the viral load in the lungs of SARS-CoV-

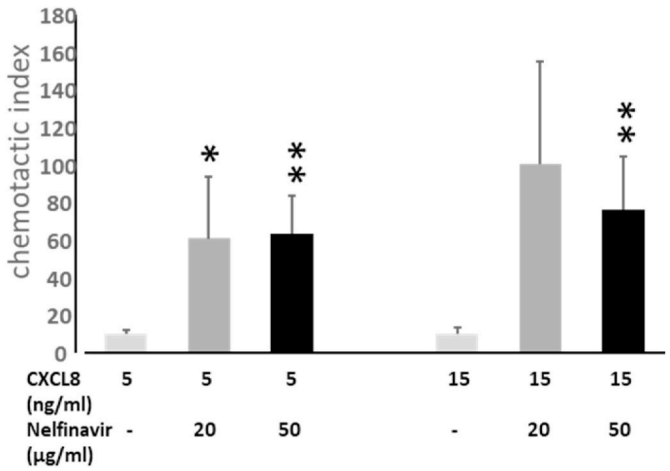

Fig. 4. The migration of human neutrophils towards CXCL8 is enhanced in the presence of Nelfinavir.

2-infected hamsters, yet surprisingly, it markedly improves lung pathology. The lack of antiviral efficacy observed here is consistent with preliminary data reported from another study in which Nelfinavir was administered orally at a dose of 250 mg/kg/day BID (boosted with Ritonavir) for two consecutive days followed by sacrifice on day 3 post-infection (Nougairede et al., 2020). No significant reduction of viral RNA or infectious virus titres was observed in the lungs of hamsters in this study (Nougairede et al., 2020). In contrast, another study in which SARS-CoV-2-infected hamsters were orally treated with a dose of 30 mg/kg/day BID of Nelfinaivir for three days with sacrifice on day 3 post-infection (Jan et al., 2021) demonstrated a small (0.5 $\log_{10}$) but significant reduction in lung viral titres in the Nelfinavir-treated group. It is possible that these differences in measured antiviral efficacies of Nelfinavir in hamsters arise from the different SARS-CoV-2 strains and inoculum in the studies. However, histopathological analyses were not discussed in either study.

We here also observe a marked infiltration of neutrophils in the lungs and an increase in blood neutrophil levels as studied in uninfected hamsters treated with Nelfinavir. Due to limitations in reagents for performing assays with hamster neutrophils, clinically relevant human neutrophils were used as a surrogate to further investigate the effects of Nelfinavir. While typical markers of neutrophil activation (changes in degranulation markers, adhesion molecules, or chemoattractant receptors) were not detected in human neutrophils in the presence of Nelfinavir, an enhanced chemotactic response of human neutrophils to the CXC chemokine CXCL8 was observed. The observations made in the studies with human and hamster neutrophils may indicate an immunomodulatory effect associated with Nelfinavir treatment, the exact underlying mechanisms of which remain to be further investigated in both species. In hamsters, this immunomodulatory effect is likely to account for the substantial improvement in SARS-CoV-2-induced lung pathology despite the lack of effect on viral load. In addition to Nelfinavir, there are currently seven other FDA-approved protease inhibitors which are used as part of highly active antiretroviral therapy (HAART) for HIV treatment, namely atazanavir, darunavir, fosamprenavir, indinavir, lopinavir/ritonavir, saquinavir and tipranavir ("Antiretroviral Therapy for HIV Infection, 2021). An improvement in $CD4^+$ T-cell counts and clinical status have been reported in HIV patients treated with protease inhibitors even without viral load suppression (Kaufmann et al., 1998; Lecossier et al., 2001; Levitz, 1998; Meroni et al., 2002; Piketty et al., 1998, 2001). This has been attributed to the fact that apart from their antiviral activity, some of these PIs exert multiple effects on various cellular processes, including apoptosis and immune cell functions (Gaedicke et al., 2002; Ghibelli et al., 2003; Gruber et al., 2001; Mastroianni et al., 2000). For instance, HIV protease inhibitors (nelfinavir, indinavir, ritonavir) were reported to reduce apoptosis, correlating with an increased chemotactic function of polymorphonuclear leukocytes *in vitro* and *ex vivo* from treated HIV-infected patients (Mastroianni et al., 2000). This includes patients who have a sustained increase in $CD4^+$ T-cell count without a concomitant decline in HIV load. These findings, in the context of HIV infections, lend support to the intriguing observations made in our study.

The most common adverse effect of Nelfinavir treatment in humans is gastrointestinal intolerance (Perry et al., 2005), which we have likewise observed from gastrointestinal incidents in the hamsters in these studies. Nelfinavir (Viracept) has been withdrawn from use in the European Union, although it is still in use in the US as an FDA-approved drug ("Drugs@FDA," n.d.; European Medicines Agency, 2018). Lopinavir/Ritonavir (Kaletra™) is a widely-used HIV protease inhibitor intended as fixed combination therapy for HIV. Despite *in vitro* activity against SARS-CoV-2 (Choy et al., 2020), Kaletra™ did not result in a beneficial effect in patients hospitalized for COVID-19 (>8000 patients in completed trials) (Cao et al., 2020; Consortium, 2020; "Lopinavir–ritonavir in patients admitted to hospital with COVID-19 (RECOVERY): a randomised, controlled, open-label, platform trial - ScienceDirect," n.d.). Whether it may be effective in preventing progression of mild COVID-19 when treatment is initiated early after the onset of symptoms is being evaluated in ongoing clinical trials in non-hospitalized patients (NCT04372628, NCT04403100 - both studies currently - 29th November 2021 - recruiting) ("Home - ClinicalTrials.gov," n.d.).

The lack of a protective activity in hospitalized COVID19 patients may be because of an already too fulminant pathology. Also the dosing of Lopinavir/Ritonavir may be inadequate (Karolyi et al., 2021). The median Lopinavir steady state plasma concentration in COVID-19 patients was 13.6 µg/ml when the standard dosing regimen of Lopinavir/Ritonavir for HIV treatment was used (400/100 mg, BID) (Schoergenhofer et al., 2020), which is less than the EC50 of 16.4 µg/ml for SARS-CoV-2 (Choy et al., 2020). In our study, a dose of 80/20 mg/kg of Lopinavir/Ritonavir was used based on the human equivalent dose normalised to the hamster body surface area (Reagan-Shaw et al., 2008). An average Lopinavir plasma concentration of 275 nM (0.17 µg/ml) was measured about 24 h after the last dose, which is about a 100-fold less than the steady state concentration observed in humans. In the case of Nelfinavir, for a standard dosing regimen of either 1250 mg BID or 750 mg TID, trough Nelfinavir levels in HIV patients are between 1 and 2.2 µg/ml as indicated by the manufacturer (La Jolla, CA: Agouron, 1998), although larger variations from 0.1 to 11.7 µg/ml were reported (Marzolini et al., 2001). While a human equivalent dose of Nelfinavir was not used in our study as weight loss and signs of diarrhoea were observed at 50 mg/kg BID, an average Nelfinavir plasma concentration of 170 nM (0.11 µg/ml) was measured about 16 h after the last dose, which is in the lower range observed in humans (Ianevski et al., 2020). In spite of not achieving the same plasma levels as measured in humans, both Nelfinavir and Lopinavir/Ritonavir demonstrated an effect by significantly improving SARS-CoV-2-induced lung pathology in hamsters.

5. Conclusion

The clear beneficial effect of the Lopinavir/Ritonavir combination as observed in the hamster model warrants further exploration of the effect of this combination in humans with COVID19. It is hoped that in the clinical trials (NCT04372628, NCT04403100) in non-hospitalized patients (studies in the recruiting phase) a beneficial effect of the treatment will be noted. We will explore the effect of other HIV protease inhibitors in the hamster model as well as the combined effect with directly-acting antivirals (such as Molnupiravir and Paxlovid™).

Funding

The Bill & Melinda Gates Foundation (BGMF) under grant agreement

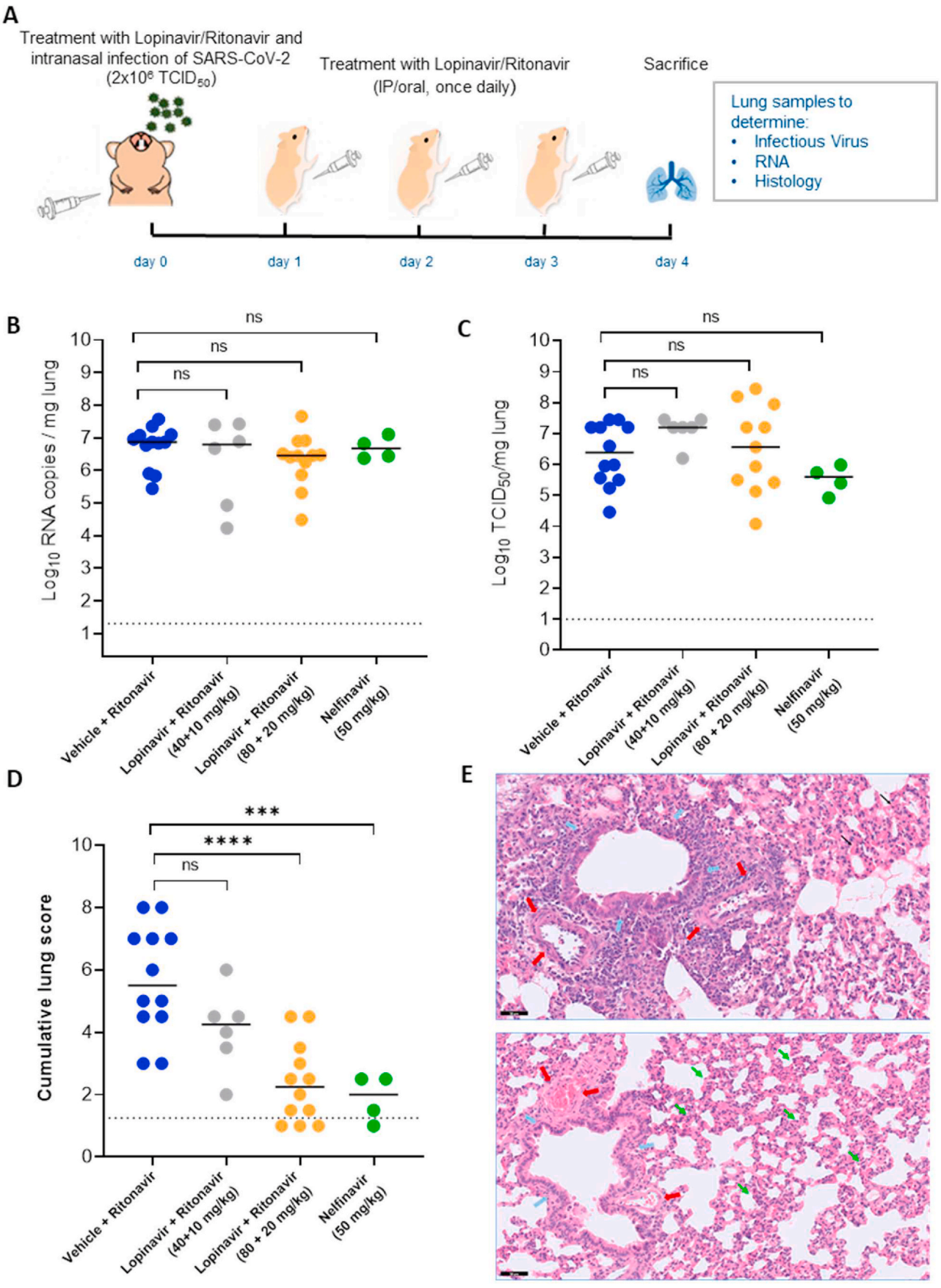

(caption on next page)

Fig. 5. Lopinavir/Ritonavir improve lung pathology of SARS-CoV-2-infected Syrian hamsters despite lack of an antiviral effect. (A) Set-up of the study. **(B)** Viral RNA levels in the lungs of hamsters treated with vehicle/Ritonavir (20 mg/kg, once daily) (control), Lopinavir/Ritonavir (40/10 mg/kg once daily), Lopinavir/Ritonavir (80/20 mg/kg once daily), or 50 mg/kg Nelfinavir BID at 4 dpi expressed as $\log_{10}$ SARS-CoV-2 RNA copies per mg lung tissue. Individual data and median values are presented. **(C)** Infectious virus titres in the lungs of hamsters treated with vehicle/Ritonavir (20 mg/kg, once daily), Lopinavir/Ritonavir (40/10 mg/kg once daily), Lopinavir/Ritonavir (80/20 mg/kg once daily), or 50 mg/kg Nelfinavir BID at 4 dpi expressed as $\log_{10}$ $TCID_{50}$ per mg lung tissue. Individual data and median values are presented. **(D)** Cumulative severity score from H&E-stained slides of lungs from SARS-CoV-2-infected hamsters at 4 dpi treated with vehicle/Ritonavir (20 mg/kg, once daily), Lopinavir/Ritonavir (40/10 mg/kg once daily), Lopinavir/Ritonavir (80/20 mg/kg once daily), or 50 mg/kg Nelfinavir BID. Individual datapoints and lines indicating median values are presented. The dotted line represents the median lung score in healthy, untreated, non-infected animals. (E) Representative H&E-stained slides of lungs from vehicle/Ritonavir (20 mg/kg, once daily) (top panel) and Lopinavir/Ritonavir (80/20 mg/kg once daily) (bottom panel) SARS-CoV-2-infected hamsters at 4 dpi. Top panel: Peri-bronchial (blue arrows) and perivascular inflammation (red arrows) with endothelialitis in a vehicle/Ritonavir-treated hamster. Interstitium is congestive (scale bar at 50 μm). Bottom panel: No peri-bronchial (blue arrows) or peri-vascular (red arrows) inflammation, but presence of interstitial neutrophils (green arrows) in a Lopinavir/Ritonavir-treated hamster (scale bar at 50 μm). Data are from two independent studies (12 hamsters per group for vehicle/Ritonavir, 6 for Lopinavir/Ritonavir (40/10 mg/kg), 12 for Lopinavir/Ritonavir (80/20 mg/kg), and 4 hamsters for Nelfinavir). Data were analyzed using the Mann-Whitney *U* test. ns indicates non-significant; $^{**}P < 0.01$.

INV-00636. Covid-19-Fund KU Leuven/UZ Leuven and the COVID-19 call of FWO-Vlaanderen (G0G4820N). The European Union's Horizon 2020 research and innovation program under grant agreements No. 101003627 (SCORE project).

SC received a PhD fellowship and JV a senior postdoctoral fellowship of FWO-Vlaanderen.

CSF, RA, LL were supported by a KU Leuven internal project fund

XZ received funding of the China Scholarship Council (grant No.201906170033).

Declaration of competing interest

None to declare.

Acknowledgements

We thank Carolien De Keyzer, Lindsey Bervoets, Thibault Francken, Elke Maas, Jasper Rymenants, Birgit Voeten, Dagmar Buyst, Niels Cremers, Bo Corbeels and Kathleen Van den Eynde for excellent technical assistance. We are grateful to Piet Maes for kindly providing the SARS-CoV-2 strain used in this study. We thank Jef Arnout and Annelies Sterckx (KU Leuven Faculty of Medicine, Biomedical Sciences Group Management) and the Animalia and Biosafety Departments of KU Leuven for facilitating the animal studies. We thank Monalisa Chatterji, Fran Berlioz-Seux, Robert Jordan, and Betsy Russell for insightful and helpful discussions. We thank all healthy volunteers who donated blood samples.

Appendix A. Supplementary data

Supplementary data to this article can be found online at https://doi.org/10.1016/j.antiviral.2022.105311.

(A) Set-up of the study. **(B–G)** Parameters from the automated hematological analysis of whole blood from non-infected hamsters treated with either vehicle control or 50 mg/kg Nelfinavir BID at 4 dpi. (B) White blood cell count; (C) Platelet count; (D) Neutrophil count; (E) Neutrophil granularity index (Neut-GI); (F) Neutrophil reactivity index (Neut-RI); (G) Neutrophil forward scatter (Neut-FSC). Data obtained were from two independent experiments ($n = 8$ for vehicle with 3 excluded samples for panels B–D due to blood clot formation; $n = 9$ for Nelfinavir with 1 excluded sample for panels B–D due to blood clot formation). Data were analyzed using the Mann-Whitney *U* test. ns indicates non-significant, $^{*}P < 0.05$, $^{**}P < 0.01$, $^{***}P < 0.001$.

Recombinant CXCL8 (5 or 15 ng/ml) was added to the lower compartment of the Boyden microchamber. Freshly isolated human neutrophils in the presence of vehicle control or nelfinavir (20 or 50 μg/ml) were added to the upper compartment and allowed to migrate for 45 min at 37 °C. The chemotactic potencies are expressed as mean chemotactic index (±SEM) derived from 5 independent experiments with neutrophils from different healthy donors. Statistically significant differences between chemotactic responses in the presence or absence of Nelfinavir were calculated with the Mann-Whitney test and are indicated by asterisks ($^{*}P < 0.05$; $^{**}P < 0.01$).

References

Abdelnabi, R., Foo, C.S., De Jonghe, S., Maes, P., Weynand, B., Neyts, J., 2021. Molnupiravir inhibits replication of the emerging SARS-CoV-2 variants of concern in a hamster infection model. J. Infect. Dis. 224, 749–753. https://doi.org/10.1093/infdis/jiab361.

Antiretroviral Therapy for HIV Infection: Overview, 2021. FDA-approved Antivirals and Regimens. Complete Regimen Combination ARTs.

Bolcato, G., Bissaro, M., Pavan, M., Sturlese, M., Moro, S., 2020. Targeting the coronavirus SARS-CoV-2: computational insights into the mechanism of action of the protease inhibitors lopinavir, ritonavir and nelfinavir. Sci. Rep. 10, 20927. https://doi.org/10.1038/s41598-020-77700-z.

Boudewijns, R., Thibaut, H.J., Kaptein, S.J.F., Li, R., Vergote, V., Seldeslachts, L., Van Weyenbergh, J., De Keyzer, C., Bervoets, L., Sharma, S., Liesenborghs, L., Ma, J., Jansen, S., Van Looveren, D., Vercruysse, T., Wang, X., Jochmans, D., Martens, E., Roose, K., De Vlieger, D., Schepens, B., Van Buyten, T., Jacobs, S., Liu, Y., Martí-Carreras, J., Vanmechelen, B., Wawina-Bokalanga, T., Delang, L., Rocha-Pereira, J., Coelmont, L., Chiu, W., Leyssen, P., Heylen, E., Schols, D., Wang, L., Close, L., Matthijnssens, J., Van Ranst, M., Compernolle, V., Schramm, G., Van Laere, K., Saelens, X., Callewaert, N., Opdenakker, G., Maes, P., Weynand, B., Cawthorne, C., Vande Velde, G., Wang, Z., Neyts, J., Dallmeier, K., 2020. STAT2 signaling restricts viral dissemination but drives severe pneumonia in SARS-CoV-2 infected hamsters. Nat. Commun. 11 https://doi.org/10.1038/s41467-020-19684-y.

Cao, B., Wang, Y., Wen, D., Liu, W., Wang, J., Fan, G., Ruan, L., Song, B., Cai, Y., Wei, M., Li, X., Xia, J., Chen, N., Xiang, J., Yu, T., Bai, T., Xie, X., Zhang, L., Li, C., Yuan, Y., Chen, H., Li, H., Huang, H., Tu, S., Gong, F., Liu, Y., Wei, Y., Dong, C., Zhou, F., Gu, X., Xu, J., Liu, Z., Zhang, Y., Li, H., Shang, L., Wang, K., Li, K., Zhou, X., Dong, X., Qu, Z., Lu, S., Hu, X., Ruan, S., Luo, S., Wu, J., Peng, L., Cheng, F., Pan, L., Zou, J., Jia, C., Wang, J., Liu, X., Wang, S., Wu, X., Ge, Q., He, J., Zhan, H., Qiu, F., Guo, L., Huang, C., Jaki, T., Hayden, F.G., Horby, P.W., Zhang, D., Wang, C., 2020. A trial of lopinavir–ritonavir in adults hospitalized with severe Covid-19. N. Engl. J. Med. NEJMoa2001282. https://doi.org/10.1056/NEJMoa2001282.

Choy, K.-T., Wong, A.Y.-L., Kaewpreedee, P., Sia, S.F., Chen, D., Hui, K.P.Y., Chu, D.K.W., Chan, M.C.W., Cheung, P.P.-H., Huang, X., Peiris, M., Yen, H.-L., 2020. Remdesivir, lopinavir, emetine, and homoharringtonine inhibit SARS-CoV-2 replication in vitro. Antivir. Res. 178, 104786. https://doi.org/10.1016/j.antiviral.2020.104786.

Chu, C., Cheng, V., Hung, I., Wong, M., Chan, K., Chan, K., Kao, R., Poon, L., Wong, C., Guan, Y., Peiris, J., Yuen, K., 2004. Role of lopinavir/ritonavir in the treatment of SARS: initial virological and clinical findings. Thorax 59, 252–256. https://doi.org/10.1136/thorax.2003.012658.

Consortium, W.S.T., 2020. Repurposed antiviral drugs for Covid-19 — interim WHO solidarity trial results. N. Engl. J. Med. https://doi.org/10.1056/NEJMoa2023184.

de Wilde, A.H., Jochmans, D., Posthuma, C.C., Zevenhoven-Dobbe, J.C., van Nieuwkoop, S., Bestebroer, T.M., van den Hoogen, B.G., Neyts, J., Snijder, E.J., 2014. Screening of an FDA-approved compound library identifies four small-molecule inhibitors of Middle East respiratory syndrome coronavirus replication in cell culture. Antimicrob. Agents Chemother. 58, 4875–4884. https://doi.org/10.1128/AAC.03011-14.

Drugs@FDA: FDA-approved Drugs ([WWW Document], n.d).

European Medicines Agency, 2018. Viracept. Eur. Med. Agency [WWW Document].

Gaedicke, S., Firat-Geier, E., Constantiniu, O., Lucchiari-Hartz, M., Freudenberg, M., Galanos, C., Niedermann, G., 2002. Antitumor effect of the human immunodeficiency virus protease inhibitor ritonavir: induction of tumor-cell apoptosis associated with perturbation of proteasomal proteolysis. Cancer Res. 62, 6901–6908.

Ghibelli, L., Mengoni, F., Lichtner, M., Coppola, S., De Nicola, M., Bergamaschi, A., Mastroianni, C., Vullo, V., 2003. Anti-apoptotic effect of HIV protease inhibitors via direct inhibition of calpain. Biochem. Pharmacol. 66, 1505–1512. https://doi.org/10.1016/s0006-2952(03)00505-7.

Gruber, A., Wheat, J.C., Kuhen, K.L., Looney, D.J., Wong-Staal, F., 2001. Differential effects of HIV-1 protease inhibitors on dendritic cell immunophenotype and function. J. Biol. Chem. 276, 47840–47843. https://doi.org/10.1074/jbc.M105582200.

Home - ClinicalTrials.Gov [WWW Document], n.d.
Huynh, T., Wang, H., Luan, B., 2020. In silico exploration of the molecular mechanism of clinically oriented drugs for possibly inhibiting SARS-CoV-2's main protease. J. Phys. Chem. Lett. 11, 4413–4420. https://doi.org/10.1021/acs.jpclett.0c00994.
Ianevski, A., Yao, R., Fenstad, M.H., Biza, S., Zusinaite, E., Reisberg, T., Lysvand, H., Løseth, K., Landsem, V.M., Malmring, J.F., Oksenych, V., Erlandsen, S.E., Aas, P.A., Hagen, L., Pettersen, C.H., Tenson, T., Afset, J.E., Nordbø, S.A., Bjørås, M., Kainov, D. E., 2020. Potential antiviral options against SARS-CoV-2 infection. Viruses 12, 642. https://doi.org/10.3390/v12060642.
Jan, J.-T., Cheng, T.-J.R., Juang, Y.-P., Ma, H.-H., Wu, Y.-T., Yang, W.-B., Cheng, C.-W., Chen, X., Chou, T.-H., Shie, J.-J., Cheng, W.-C., Chein, R.-J., Mao, S.-S., Liang, P.-H., Ma, C., Hung, S.-C., Wong, C.-H., 2021. Identification of existing pharmaceuticals and herbal medicines as inhibitors of SARS-CoV-2 infection. Proc. Natl. Acad. Sci. Unit. States Am. 118 https://doi.org/10.1073/pnas.2021579118.
Kaldor, S.W., Kalish, V.J., Davies, J.F., Shetty, B.V., Fritz, J.E., Appelt, K., Burgess, J.A., Campanale, K.M., Chirgadze, N.Y., Clawson, D.K., Dressman, B.A., Hatch, S.D., Khalil, D.A., Kosa, M.B., Lubbehusen, P.P., Muesing, M.A., Patick, A.K., Reich, S.H., Su, K.S., Tatlock, J.H., 1997. Viracept (nelfinavir mesylate, AG1343): a potent, orally bioavailable inhibitor of HIV-1 protease. J. Med. Chem. 40, 3979–3985. https://doi.org/10.1021/jm9704098.
Kaplan, A.H., Zack, J.A., Knigge, M., Paul, D.A., Kempf, D.J., Norbeck, D.W., Swanstrom, R., 1993. Partial inhibition of the human immunodeficiency virus type 1 protease results in aberrant virus assembly and the formation of noninfectious particles. J. Virol. 67, 4050–4055. https://doi.org/10.1128/JVI.67.7.4050-4055.1993.
Kaptein, S.J.F., Jacobs, S., Langendries, L., Seldeslachts, L., ter Horst, S., Liesenborghs, L., Hens, B., Vergote, V., Heylen, E., Barthelemy, K., Maas, E., de Keyzer, C., Bervoets, L., Rymenants, J., van Buyten, T., Zhang, X., Abdelnabi, R., Pang, J., Williams, R., Thibaut, H.J., Dallmeier, K., Boudewijns, R., Wouters, J., Augustijns, P., Verougstraete, N., Cawthorne, C., Breuer, J., Solas, C., Weynand, B., Annaert, P., Spriet, I., Velde, Vande, G., Neyts, J., Rocha-Pereira, J., Delang, L., 2020. Favipiravir at high doses has potent antiviral activity in SARS-CoV-2−infected hamsters, whereas hydroxychloroquine lacks activity. Proc. Natl. Acad. Sci. U. S. A 117, 26955–26965. https://doi.org/10.1073/pnas.2014441117.
Karolyi, M., Omid, S., Pawelka, E., Jilma, B., Stimpfl, T., Schoergenhofer, C., Laferl, H., Seitz, T., Traugott, M., Wenisch, C., Zoufaly, A., 2021. High dose lopinavir/ritonavir does not lead to sufficient plasma levels to inhibit SARS-CoV-2 in hospitalized patients with COVID-19. Front. Pharmacol. 12, 704767. https://doi.org/10.3389/fphar.2021.704767.
Kaufmann, D., Pantaleo, G., Sudre, P., Telenti, A., 1998. CD4-cell count in HIV-1-infected individuals remaining viraemic with highly active antiretroviral therapy (HAART). Swiss HIV Cohort Study. Lancet (London, England) 351, 723–724. https://doi.org/10.1016/s0140-6736(98)24010-4.
Kempf, D.J., Marsh, K.C., Kumar, G., Rodrigues, A.D., Denissen, J.F., McDonald, E., Kukulka, M.J., Hsu, A., Granneman, G.R., Baroldi, P.A., Sun, E., Pizzuti, D., Plattner, J.J., Norbeck, D.W., Leonard, J.M., 1997. Pharmacokinetic enhancement of inhibitors of the human immunodeficiency virus protease by coadministration with ritonavir. Antimicrob. Agents Chemother. 41, 654–660. https://doi.org/10.1128/AAC.41.3.654.
La Jolla, CA: Agouron, 1998. Product information. Viracept (nelfinavir).
Lecossier, D., Bouchonnet, F., Schneider, P., Clavel, F., Hance, A.J., 2001. Discordant increases in CD4+ T cells in human immunodeficiency virus-infected patients experiencing virologic treatment failure: role of changes in thymic output and T cell death. J. Infect. Dis. 183, 1009–1016. https://doi.org/10.1086/319285.
Levitz, S.M., 1998. Improvement in CD4+ cell counts despite persistently detectable HIV load. N. Engl. J. Med. 338, 1074–1075. https://doi.org/10.1056/NEJM199804093381517.
Lopinavir–ritonavir in Patients Admitted to Hospital with COVID-19 (RECOVERY): a Randomised, Controlled, Open-Label, Platform Trial - ScienceDirect [WWW Document], n.d.
Marzolini, C., Buclin, T., Decosterd, L.A., Biollaz, J., Telenti, A., 2001. Nelfinavir plasma levels under twice-daily and three-times-daily regimens: high interpatient and low intrapatient variability. Ther. Drug Monit. 23, 394–398. https://doi.org/10.1097/00007691-200108000-00012.
Mastroianni, C.M., Mengoni, F., Lichtner, M., D'Agostino, C., d'Ettorre, G., Forcina, G., Marzi, M., Russo, G., Massetti, A.P., Vullo, V., 2000. Ex vivo and in vitro effect of human immunodeficiency virus protease inhibitors on neutrophil apoptosis. J. Infect. Dis. 182, 1536–1539. https://doi.org/10.1086/315858.
Meroni, L., Varchetta, S., Manganaro, D., Gatti, N., Riva, A., Monforte, A., d'Arminio, Galli, M., 2002. Reduced levels of CD4 cell spontaneous apoptosis in human immunodeficiency virus-infected patients with discordant response to protease inhibitors. J. Infect. Dis. 186, 143–144. https://doi.org/10.1086/341075.
Metzemaekers, M., Mortier, A., Vacchini, A., Boff, D., Yu, K., Janssens, R., Farina, F.M., Milanesi, S., Berghmans, N., Pörtner, N., Van Damme, J., Allegretti, M., Teixeira, M. M., Locati, M., Borroni, E.M., Amaral, F.A., Proost, P., 2021. Endogenous modification of the chemoattractant CXCL5 alters receptor usage and enhances its activity toward neutrophils and monocytes. Sci. Signal.
Musarrat, F., Chouljenko, V., Dahal, A., Nabi, R., Chouljenko, T., Jois, S.D., Kousoulas, K. G., 2020. The anti-HIV drug nelfinavir mesylate (Viracept) is a potent inhibitor of cell fusion caused by the SARSCoV-2 spike (S) glycoprotein warranting further evaluation as an antiviral against COVID-19 infections. J. Med. Virol. 92, 2087–2095. https://doi.org/10.1002/jmv.25985.
Nougairede, A., Touret, F., Cochin, M., de Lamballerie, X., 2020. Antiviral activity of nelfinavir against SARS-CoV-2 [WWW Document]. URL. https://www.european-virus-archive.com/sites/default/files/covid19-compounds-tests/Nelfinavir.pdf, 3.16.22.
Peng, C., Ho, B.K., Chang, T.W., Chang, N.T., 1989. Role of human immunodeficiency virus type 1-specific protease in core protein maturation and viral infectivity. J. Virol. 63, 2550–2556. https://doi.org/10.1128/JVI.63.6.2550-2556.1989.
Perry, C.M., Frampton, J.E., McCormack, P.L., Siddiqui, M.A.A., Cvetković, R.S., 2005. Nelfinavir. Drugs 65, 2209–2244. https://doi.org/10.2165/00003495-200565150-00015.
Piketty, C., Castiel, P., Belec, L., Batisse, D., Si Mohamed, A., Gilquin, J., Gonzalez-Canali, G., Jayle, D., Karmochkine, M., Weiss, L., Aboulker, J.P., Kazatchkine, M.D., 1998. Discrepant responses to triple combination antiretroviral therapy in advanced HIV disease. AIDS 12, 745–750. https://doi.org/10.1097/00002030-199807000-00011.
Piketty, C., Weiss, L., Thomas, F., Mohamed, A.S., Belec, L., Kazatchkine, M.D., 2001. Long-term clinical outcome of human immunodeficiency virus-infected patients with discordant immunologic and virologic responses to a protease inhibitor-containing regimen. J. Infect. Dis. 183, 1328–1335. https://doi.org/10.1086/319861.
Reagan-Shaw, S., Nihal, M., Ahmad, N., 2008. Dose translation from animal to human studies revisited. Faseb. J. 22, 659–661. https://doi.org/10.1096/fj.07-9574LSF.
Reed, L.J., Muench, H., 1938. A simple method of estimating fifty percent endpoints. Am. J. Hyg. 27, 493–497. https://doi.org/10.1016/j.jvs.2011.05.096.
Schoergenhofer, C., Jilma, B., Stimpfl, T., Karolyi, M., Zoufaly, A., 2020. Pharmacokinetics of lopinavir and ritonavir in patients hospitalized with coronavirus disease 2019 (COVID-19). Ann. Intern. Med. M20–1550 https://doi.org/10.7326/M20-1550.
Sham, H.L., Kempf, D.J., Molla, A., Marsh, K.C., Kumar, G.N., Chen, C.-M., Kati, W., Stewart, K., Lal, R., Hsu, A., Betebenner, D., Korneyeva, M., Vasavanonda, S., McDonald, E., Saldivar, A., Wideburg, N., Chen, X., Niu, P., Park, C., Jayanti, V., Grabowski, B., Granneman, G.R., Sun, E., Japour, A.J., Leonard, J.M., Plattner, J.J., Norbeck, D.W., 1998. ABT-378, a highly potent inhibitor of the human immunodeficiency virus protease. Antimicrob. Agents Chemother. 42, 3218–3224. https://doi.org/10.1128/AAC.42.12.3218.
Tay, M.Z., Poh, C.M., Rénia, L., MacAry, P.A., Ng, L.F.P., 2020. The trinity of COVID-19: immunity, inflammation and intervention. Nat. Rev. Immunol. https://doi.org/10.1038/s41577-020-0311-8.
WHO Coronavirus Disease, 2022. COVID-19) Dashboard. WWW Document].
Xu, Z., Peng, C., Shi, Y., Zhu, Z., Mu, K., Wang, X., Zhu, W., 2020. Nelfinavir was predicted to be a potential inhibitor of 2019-nCov main protease by an integrative approach combining homology modelling, molecular docking and binding free energy calculation. bioRxiv. https://doi.org/10.1101/2020.01.27.921627, 2020.01.27.921627.
Yamamoto, N., Matsuyama, S., Hoshino, T., Yamamoto, N., 2020. Nelfinavir inhibits replication of severe acute respiratory syndrome coronavirus 2 in vitro. bioRxiv. https://doi.org/10.1101/2020.04.06.026476, 2020.04.06.026476.